

## Superstable Granular Heap in a Thin Channel

Nicolas Taberlet,<sup>1,2</sup> Patrick Richard,<sup>1</sup> Alexandre Valance,<sup>1</sup> Wolfgang Losert,<sup>2</sup> José Miguel Pasini,<sup>3</sup>  
James T. Jenkins,<sup>3</sup> and Renaud Delannay<sup>1</sup>

<sup>1</sup>*GMCM, Université Rennes 1, Batiment 11A, 35042 Rennes, France*

<sup>2</sup>*IREAP, Department of Physics, University of Maryland, College Park, Maryland 20742, USA*

<sup>3</sup>*Department of Theoretical and Applied Mechanics, Cornell University, Ithaca, New York 14853, USA*

(Received 25 July 2003; published 24 December 2003)

We observed experimentally a new regime for granular flows in an inclined channel with a flow-rate-controlled system. For high flow rates, the flow occurs atop a static granular heap whose angle is considerably higher than those usually exhibited by granular heaps. The properties of such superstable heaps (SSH) are drastically affected by a change in the channel width  $W$ . This indicates that the unusual stability of these heaps can be accounted for by the flowing layer and its friction on the sidewalls. A simple depth-averaged model, assuming Coulomb friction, shows that the SSH angle scales as  $h/W$  ( $W$  being the channel width), and that grain size plays no part.

DOI: 10.1103/PhysRevLett.91.264301

PACS numbers: 45.70.Ht, 05.45.Yv, 45.70.Cc, 47.60.+i

Granular flows can exhibit various behaviors, ranging from a gaslike to a solidlike state. Such flows are encountered in geology, since debris flows, rock avalanches, and pyroclastic flows consist of individual grains [1,2], as well as in industrial applications (cereal transport, powder mixing). Much experimental [3–5], numerical [6,7], as well as theoretical [8] work was devoted to the understanding of these flows but developing predictive models still remains a challenge. Previous experimental work on granular flows down inclines can be classified in two different categories: height-controlled flows [4,7] and flow-rate-controlled flows [1,3,9]. In the former, the sand is released from a reservoir through a gate, hence controlling the input height whereas, in the latter, the sand is directly released from a reservoir onto the incline, hence controlling the flow rate. In both configurations steady and fully developed flows (SFD) can be observed for a given range of tilt angles and heights (or flow rates). Such flows are characterized by a height and velocity profile which are constant in both time and space. A previous study [10] demonstrated that height-controlled and flow-rate-controlled systems produce the same results only for a limited range of parameters.

In the present study, a flow-rate-controlled system was used: Granular material was poured from a hopper into an open three-dimensional channel. Within this geometry, we discovered a new regime in which the flow occurs atop a stabilized static heap. This heap forms spontaneously and its angle can be very high [see Fig. 1(a)], much greater than the angle of repose. We present here an experimental study of such flows and propose a simple depth-averaged model that describes the observed phenomenon. The model shows, in particular, that the superstable heap (SSH) is stabilized by the flowing layer atop it and emphasizes the key role of the sidewall friction on the flowing material. Moreover, the model furnishes a simple linear relation between the SSH angle and  $h/W$  (where  $W$

is the channel width and  $h$  the height of the flowing layer), which is confirmed experimentally. This points out that, at least in the range of our measurements, the relevant parameter to characterize the effect of the wall friction on the flow is  $h/W$ , and that the grain size plays no part.

Our experimental setup consists of a thin three-dimensional 50-cm-long open channel that could be inclined from horizontal to an angle  $\theta$  [Fig. 1(b)]. Although  $\theta$  could range from  $0^\circ$  to  $90^\circ$ , our experiments were conducted in a steep configuration in which  $\theta$  was always set to be higher than the angle at which all the grains flow out of the channel after the feeding is cut off. Experiments were performed with both dry polydisperse beach sand (0.1–0.8 mm) and slightly polydisperse glass beads (0.6–0.9 mm). Granular material was continuously poured on a rough bottom placed between two transparent vertical glass plates through a hopper whose aperture precisely controlled the input flow rate  $Q_{\text{in}}$  defined as the mass of

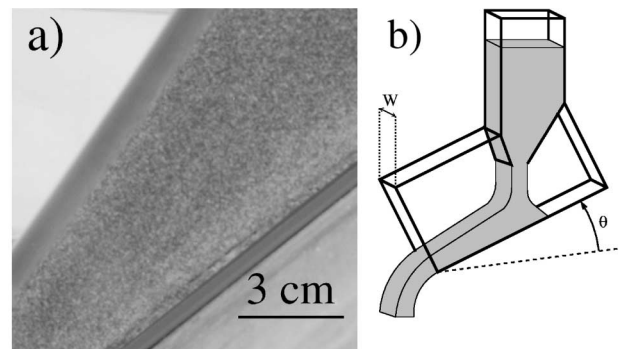


FIG. 1. (a) Snapshot of flowing sand taken with a regular video camera with  $1/30$  s exposure time. The blurry part corresponds to flowing grains and the sharp part is static. (b) Sketch of the experimental setup. The granular material is poured from a hopper onto a rough bottom between two vertical plates.

material entering the channel per unit of time and per unit of width [ $Q_{in} = \text{mass}/(\text{time} \times W)$ ]. The rough bottom was made of grains (sand or glass beads) glued to a flat rigid substrate. The gap between the two vertical plates  $W$  was varied from 5 mm up to 2 cm. The opening of the hopper was placed 20 cm above the rough bottom, avoiding any feedback interaction between the input flow and the flow in the channel, therefore allowing the feeding rate,  $Q_{in}$ , to be tunable and to remain constant throughout an experimental run. All our experiments were conducted in a temperature and humidity-controlled room (24° and 55% humidity). In order to minimize electrostatic effects, the material was passed through a metal sieve connected to the ground prior to all experiments. The angles were measured using an image processing software, leading to a 0.2° uncertainty. The output flow rate,  $Q_{out}$ , was determined using an electronic scale which weighed the material falling out of the channel. A fast camera took pictures at the rate of 8000 frames per second which allowed us to perform particle tracking.

In our system, we found that, for a wide range of parameters (to be specified later on), when granular material is poured from the hopper, a static heap slowly forms by trapping grains at its top. After a transient, the growth of the heap eventually stops and the flow at its surface reaches a steady state. A curved shape of the heap is observed in the region close to the point where the grains, free falling from the hopper, merge into the flowing layer. It is followed by a large region where the height of the free surface of the flow with respect to the channel bottom is found to decrease linearly with the position in the channel. Near the exit of the channel, we also observe a small region (over a typical length of 20 particle diameters) in which particles accelerate down the slope before free falling out.

A sketch representing the velocity profiles taken at different positions along the flow is shown in Fig. 2(a). They consist of a linear part of some tens of particle diameters and then smoothly decreases to zero. This allows us to draw a simple picture of the phenomenon [Fig. 2(b)] with two kinds of population: one consisting of moving grain in the first layers from the surface, and

another consisting of quasi-immobile grains in deeper parts of the pile. The  $(x, y, z)$  axes are defined as shown in Fig. 2(b):  $x$  is the direction along the flow,  $y$  is perpendicular to the surface, and  $z$  is perpendicular to the sidewall.

The remarkable feature exhibited by these static heaps is that their angle relative to the horizontal  $\varphi$  can be very high (up to 60° in our experiments). Therefore such heaps will be referred to as SSH. Note that these SSHs occur even though the channel is steep enough to let any classic heap flows out of the system. Hence, SSHs must be dynamically stabilized by the material flowing atop them. Indeed, when the system is no longer fed with sand, the SSH then falls apart and evacuates the channel. Similar features were observed in other flow-rate-controlled systems [9,11,12].

Note that the experimental observations are robust with respect to the type of grains as well as the dispersity (two kinds of polydisperse beach sand, polydisperse 0.8 mm glass beads, and monodisperse 0.5 mm ball bearings were used). The same qualitative behavior was also observed in a system with a smooth bottom and Plexiglas sidewalls, as well as in a purely two-dimensional geometry using polystyrene disks. Preliminary discrete element numerical simulations [13] showed good agreement with the experiments.

Figure 3 displays the velocity profile measured at the wall for a system of glass beads, at a distance of 20 cm from the channel exit. It shows a linear part on the first layers from the surface whereas, deeper in the pile, the velocity falls to small but nonzero values. In the latter region, as in flows on a static sandpile [14], the velocity was found to follow an exponential law. The leveling off at the free surface is typical of a dilute gaseous layer.

The transition between the linear part and the rest of the velocity profile is smooth, making it difficult to define a height  $h$  of the flowing layer. This height was, however, arbitrarily defined as the depth at which the tangent to the linear part intersects the  $y$  axis. The  $y$  coordinate origin was set at the depth  $h$ , so that the linear part corresponds to positive  $y$ , and the slowly decreasing part to negative  $y$ . A definition based on a velocity cutoff was also used. Both definitions provided us with identical variations of  $h$  with the parameters.

The inset of Fig. 3 displays the velocity profile at the free surface (i.e., seen from above) and shows that the flow is a plug-type flow (high slip velocity at the walls and low shear in the  $z$  direction). This indicates that the velocity measured at the wall can be identified with the actual velocity of the whole slab of material. When a SSH was observed, the height and velocity profile of the flowing layer were found to be  $x$  invariant in a large part of the channel. We found that the initial speed of the grains (i.e., the height of the hopper) can change the curvature in the transient region under the hopper but does not affect the properties of the flow in the fully developed part.

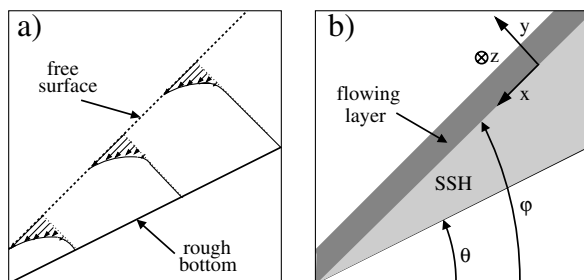


FIG. 2. Sketches of the flow. (a) Velocity profiles within the granular material. (b) Simple picture of the flow.

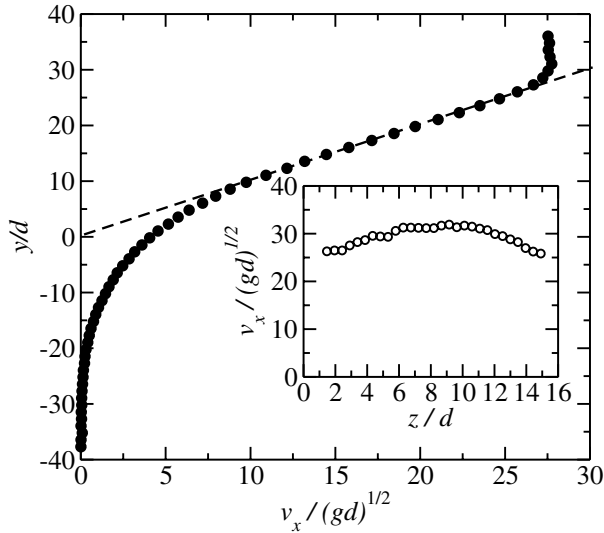


FIG. 3. Velocity profile at the wall for glass beads taken at  $x = -20$  cm for  $W = 12.5$  mm,  $Q = 90$  g s $^{-1}$  cm $^{-1}$ ,  $\theta = 40^\circ$ . The inset presents the velocity profile at the free surface.

For a given channel width  $W$ , the control parameters of our system are  $Q$  and  $\theta$ . Depending on their values, we obtain either (I) a classical SFD (or accelerated) flow on the rough bottom or (II) a flow atop a SSH. We found no hysteresis in  $\varphi(Q)$  when  $Q$  was changed during a run. The type of flow was determined by analyzing the velocity profiles taken at different positions in the channel. As can be seen in Fig. 4(a), starting from a type-I flow, a SSH can appear when decreasing the angle of the channel, or increasing the flow rate. Note that, for the range of angle  $\theta$  explored, there always exists a corresponding critical flow rate above which SSHs appear in the channel. When the flow rate is kept constant and the angle of the channel is slowly decreased starting from a flow on the rough bottom (type-I), the characteristics of the flow change (namely, the height and velocities decrease as the packing fraction slightly increases) until a SSH gradually appears in the channel. When the angle of the channel  $\theta$  is further decreased, the angle of the SSH relative to the horizontal  $\varphi$  appears to be constant (and equal to the critical angle  $\theta$  at which the SSH first appeared). Therefore, the function  $\varphi(Q)$  is identical to the boundary line between the two phases in the  $Q - \theta$  space. Figure 4(b) is a plot of the boundary lines obtained for different values of the channel width  $W$ . These lines do not collapse, showing a dependence on the parameter  $W$ . For a given input mass flow rate per unit of width, the critical angle  $\varphi$  increases with decreasing  $W$  and the type-I region in the parameter space  $Q - \theta$  shrinks as the type-II region grows. This geometrical dependence indicates that the sidewalls of the channel play a crucial role in the phenomenon: The driving force (and thus  $\varphi$ ) has to be large enough to overcome the friction from the sidewalls so that the whole medium flows.

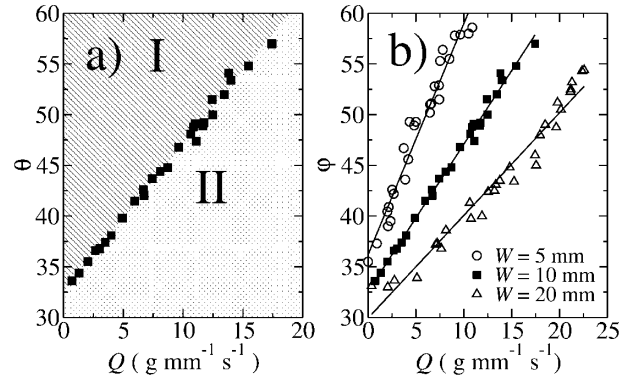


FIG. 4. Phase diagrams obtained with sand. (a) This phase diagram realized for  $W = 10$  mm shows two phases: (I) flow on the rough bottom and (II) flow atop a SSH. (b) Boundary lines between regions I and II [i.e.,  $\varphi(Q)$ ] observed for different values of the channel width  $W$ .

A simple depth-averaged model that assumes a Coulomb friction and a constant packing fraction, as reported for dense flows in many numerical simulations [7,15] and in 2D experiments [16], was used. Since we assumed a solid friction law on the walls, there is no friction force transverse to the flow direction (friction is opposed to sliding), i.e., the weight screening effect due to the presence of the sidewalls is neglected.

Moreover, assuming a fluidlike behavior, the pressure follows a hydrostatic law:  $P(y) = \rho g(h - y) \cos \varphi$ , where  $\rho$  is the constant density of the granular medium. The depth-averaged approach has been successfully used in a number of studies [8,17–19]. Since there is no gradient along  $x$ , a slab of material of height  $h$  and width  $W$ , flowing atop a static heap whose angle is  $\varphi$ , is only submitted to its weight and to the forces exerted by the SSH at the base of the flow and by sidewalls. According to Coulomb friction law, the shear stress on sidewalls is simply proportional to the depth-integrated pressure. The key of the model is that the stability condition of the SSH reads as  $S = \mu_i N$ , where  $N = \rho g h \cos \varphi$  and  $S$  are, respectively, the shear and normal stresses at the base, and  $\mu_i$  is a constant internal friction coefficient [20,10]. A SSH can grow as long as  $S < \mu_i N$ , and its angle  $\varphi$  saturates when  $S = \mu_i N$ . The force balance leads to

$$\tan \varphi = \mu_i + \mu_w \frac{h}{W}, \quad (1)$$

where  $\mu_w$  is an effective friction coefficient accounting for both sliding and rolling of the grains on the walls.

Figure 5 is a plot of  $\varphi$  vs the ratio  $h/W$ , obtained for different values of the control parameters  $Q$ ,  $\theta$ , and  $W$ . The data fall on a linear curve and then show a good agreement with Eq. (1) which indicates that, for the range of  $h/W$  (limited by technical constraints) we observed, the solid friction law on the walls seems to describe the phenomenon. For low values of  $h/d$ , the data deviates

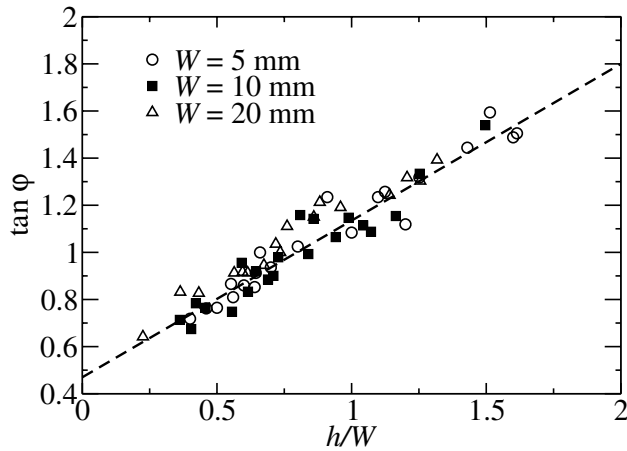


FIG. 5. The tangent of the angle  $\varphi$  is plotted as a function of the ratio  $h/W$ , for different values of the channel width  $W$  using polydisperse beach sand.

from the linear law and reaches a plateau. A best fit to the data provides us with the following values:  $\mu_i = \tan(23.3^\circ)$  and  $\mu_w = \tan(33.7^\circ)$ . This value of  $\mu_i$  is very close to those found in previous experimental and numerical studies on internal friction coefficients [21,22]. One important result of the model is that the relevant parameter to evaluate the effect of the wall friction on the flow is  $h/W$ . The model predicts an influence of the sidewall for any given channel width as long as the flowing sand layer is high enough. This last statement, however, should be tested experimentally for very large channels. One can expect the model to break down for flows in very thin channels ( $W \approx 5d$ ) where arch effects can play a crucial role. The model may also fail to describe the behavior of a flow strongly sheared in the  $z$  direction. Such a flow can be expected in a channel with very rough sidewalls.

Two points should be emphasized. First, the new regime presented here cannot be observed in a height-controlled system. Indeed, in such a system, the growth of a SSH would simply cause the grains to jam and no flow could be observed. Second, this work can explain previous results in different geometries in which high dynamic repose angles have also been observed [11,12]. In these works, the importance of the confinement due to the walls had not been pointed out by the authors.

In summary, we have experimentally studied flows in an inclined channel. We observed a new flow regime occurring at a high flow rate and characterized by the presence of a steep static heap beneath the flowing layer. Such heaps are stabilized by the material flowing atop them and fall apart when the input flow is cut off. The dependence of the phenomenon on the channel width indicates that the friction on the sidewalls plays a crucial role in the system. A depth-averaged model shows that the friction on the walls could be of great importance even in

a wide channel. The angle of these static heaps scales with  $h/W$ , and  $d$  plays no role.

The results reported here open several prospects. Using rheological models developed for granular flows, one should be able to account for the formation of the SSH and predict the variation of  $\varphi$  as a function of  $Q$  and  $W$ . Moreover, this experimental setup can be used as a rheometer since the present model indicates how one could measure the effective friction of the material flowing on the walls.

We would like to thank M. Y. Louge and J. Friedmann for helpful discussions, as well as S. Bourlès for technical assistance. This work was supported by NASA Grants No. NAG32353 and No. NAG32736, CNRS-NSF 14552, ACI catnat, and PNRN.

- 
- [1] T. G. Drake, *J. Geophys. Res.* **95**, 8681 (1990).
  - [2] J. Friedmann, *J. Sediment. Res.* **67**, 792 (1997).
  - [3] T. G. Drake, *J. Fluid Mech.* **225**, 121 (1991).
  - [4] O. Pouliquen, *Phys. Fluids* **11**, 542 (1999).
  - [5] E. Azanza, F. Chevoir, and P. Moucheront, *J. Fluid Mech.* **400**, 199 (1999).
  - [6] C. S. Campbell and P. W. Cleary, *J. Geophys. Res.* **100**, 8267 (1995).
  - [7] L. E. Silbert, D. Ertas, G. S. Grest, T. C. Halsey, D. Levine, and S. J. Plimpton, *Phys. Rev. E* **64**, 051302 (2001).
  - [8] S. B. Savage, *Theoretical and Applied Mechanics* (North-Holland, Amsterdam, 1989), p. 241; J. T. Jenkins, *Appl. Mech. Rev.* **47**, 240 (1994); K. G. Anderson and R. Jackson, *J. Fluid Mech.* **241**, 145 (1992).
  - [9] C. Ancey, *Phys. Rev. E* **65**, 011304 (2001).
  - [10] P. C. Johnson, P. Nott, and R. Jackson, *J. Fluid Mech.* **210**, 501 (2001).
  - [11] Y. Amarouchene, J. F. Boudet, and H. Kellay, *Phys. Rev. Lett.* **86**, 4286 (2001).
  - [12] D. V. Khakhar, A. V. Orpe, P. Andersen, and J. M. Ottino, *J. Fluid Mech.* **441**, 255 (2001).
  - [13] Movies and results can be found on [http://perso.univ-rennes1.fr/nicolas.taberlet/E\\_Simu.htm](http://perso.univ-rennes1.fr/nicolas.taberlet/E_Simu.htm).
  - [14] T. S. Komatsu, S. Inagaki, N. Nakagawa, and S. Nasuno, *Phys. Rev. Lett.* **86**, 1757 (2001).
  - [15] F. Chevoir, M. Prochnow, J. T. Jenkins, and P. Mills, in *Powders and Grains 2001*, edited by Y. Kishino (Balkema, Tokyo, 2001), p. 172.
  - [16] G. Berton, R. Delannay, P. Richard, N. Taberlet, and A. Valance, *Phys. Rev. E* (to be published).
  - [17] O. Pouliquen, *Phys. Fluids* **11**, 1956 (1999).
  - [18] A. W. Roberts, *Trans. ASME, J. Engng. Ind.* **91**, 373 (1969).
  - [19] S. Courrech du Pont, P. Gondret, B. Perrin, and M. Rabaud, *Europhys. Lett.* **61**, 492 (2003).
  - [20] M. Y. Louge, *Phys. Rev. E* **67**, 061303 (2003).
  - [21] R. Albert, I. Albert, D. Hornbaker, P. Schiffer, and A.-L. Barabasi, *Phys. Rev. E* **56**, R6271 (1997).
  - [22] D. Ertas, T. C. Halsey, A. J. Levine, and T. G. Mason, *Phys. Rev. E* **66**, 051307 (2002).